Radial Interaction in Dynamic Heat Transport of LHD Plasmas

S. Inagaki[1], N. Tamura[2], T. Tokuzawa[2], K. Ida[2], T. Shimozuma[2], S. Kubo[2], Y. Nagayama[2], K. Kawahata[2], S. Sudo[2], A. Komori[2], K. Itoh[1], S.-I. Itoh[1] and LHD Experimental Group.

1) Research Institute for Applied Mechanics, Kyushu University, Kasuga-Koen, Kasuga-city, Fukuoka, 816-8580, Japan
2) National Institute for Fusion Science, Oroshi-cho, Toki-shi, Gifu, 509-5292, Japan

e-mail contact of main author : inagaki@riam.kyushu-u.ac.jp

Abstract. The radial interaction of heat transport is clarified by cross-correlation between electron heat flux and electron temperature gradient in LHD. Correlations between the heat transport dynamics and the radial structures of turbulence are also investigated. The existence of a turbulence modulator is discerned by using the conventional reflectometry signals. The amplitude of high frequency (> 100kHz) density fluctuations is modulated with low frequency (< 5 kHz) in edge-core coupled plasmas. The electron cyclotron emission signals suggest the amplitude modulator has a long distance radial correlation.

1. Introduction

To understand the turbulent transport in toroidal plasmas, some models based on local turbulence led by a local micro instability have been proposed. The turbulent plasmas, however, exhibit non-local coupling. Fast propagation of the temperature perturbation has been observed, for example, by the ballistic propagation in TJ-II, the heat pulse propagation caused by L-H transition and heating power switching [1, 2, 3]. These abrupt core responses are evident before diffusive transport effects reach the core region. In addition, an abrupt core T_e rise in response to edge colling has been observed in tokamaks. These heat transport dynamics of edge-core interaction and coupling cannot be explained by the local transport models even if the heat transport is non-linear function of the temperature gradient. Thus a new perspective to turbulence transport, i.e. non-locality, has been introduced. The non-locality is also used as an explanation for turbulent transport scaling with machine size in plasma confinement studies [4, 5, 3]. Comprehensive and consistent understanding of the turbulent transport involving the non-locality is thus strongly required. Interactions of turbulence over long distances are conjectured to provide the non-local mechanism. However, turbulence structures which have the long distance correlation has not been reported. Recently, the nonlinear coupling of drift turbulence has been studied intensively. Meso-scale structure (e.g. zonal flow) is driven by microscopic turbulence [6, 7, 8, 9]. Thus, multiple spatial scale structures can coexist in turbulence. Correlations between the heat transport dynamics and the radial structures of turbulence are therefore essential to gain a comprehensive understanding of the turbulent transport. This paper presents long distance correlations between heat flux and temperature gradient and the existence of fluctuations with long radial correlation length on the order of the minor radius in LHD.

2. Transient transport experiments

The non-locality is hidden in stationary state transport and revealed in dynamic response. The cold pulse experiments in LHD (major radius R_{ax} = 3.5 m, averaged minor radius a = 0.6 m) reported in Refs.[10, 11], provide a comprehensive set of results on which dynamic patterns asso-

ciated with mechanisms for generation of non-local transport can be obtained. A cold pulse was induced using a tracer encapsulated solid pellet (TESPEL) injection [12]. The TESPEL penetrates to the region of $\rho \sim 0.8$ (ρ is the normalized radius). An abrupt core T_e rise in response to edge cooling, so-called non-local T_e rise, has been observed in LHD as well as in tokamaks [13, 14]. Typical parameters in this experiment are as follows: magnetic field at axis of 2.83T, line averaged density of $1 - 2 \times 10^{19}\mathrm{m}^{-3}$, central electron temperature of $\geq$ 1.5 keV, central ion temperature of 1-2 keV, plasma β value of 0.1%, absorbed ECH power of 0.8 MW, deposited neutral beam power of 2 MW. The experiments are performed in the low density and high temperature regime, and thus the electron loss channel is considered to be decoupled from the ion channel. The particle diffusivity is smaller than the electron heat diffusivity by one order of magnitude in this experimental conditions [15]. A 32-channel heterodyne radiometer is used to track the small electron temperature perturbations, δT_e[16].

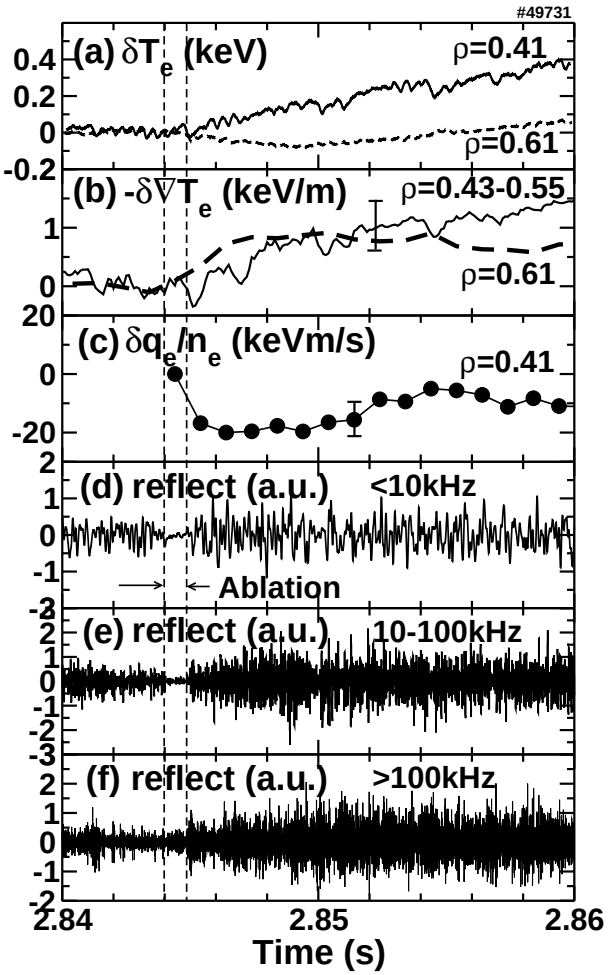

FIG. 1: Typical time evolution of (a) T_e perturbations at the normalized radius of $\rho = 0.41$ and 0.61, (b) T_e gradient at $\rho = 0.61$ and averaged in the region of $\rho = 0.43 - 0.55$, (c) heat flux perturbation at $\rho = 0.41$, (d)-(e) X-mode reflectometry signal at $\rho = 0.45$ in three different bandwidths. The time evolution of δq_e ($\rho = 0.41$) and $\delta \nabla T_e$ ($\rho = 0.61$) correlate inversely.

3. Long distance correlations between heat flux and temperature gradient

Figure 1 shows a typical time evolution of a non-local T_e rise discharge in LHD. An abrupt core temperature rise takes place in response to the TESPEL ablation. An increase in the temperature gradient, $\delta \nabla T_e$, and reduction of the heat flux, δq_e, indicate an enhancement of the core confinement. Here the δq_e is determined from the perturbed energy balance equation and can be written as,

$$\delta q_e(r,t) = \frac{1}{S} \int_0^r \frac{3}{2} n_e \frac{\partial \delta T_e}{\partial t} dV, \tag{1}$$

where S is the surface area of the closed flux surface, V is the volume. The time evolution of δq_e ($\rho = 0.41$) and $\delta \nabla T_e$ ($\rho = 0.61$) is similar (but they correlate inversely), thus the cross correlation between them is stronger than one obtained from the local δq_e - $\delta \nabla T_e$ correlation at $\rho = 0.41$. This indicates the existence of a long distance coupling of transport beyond the local turbulence correlation length. The absolute error of ∇T_e, $\delta \nabla T_e$ and δq_e determined by

the absolute calibration of electron cyclotron emission (ECE) are 20% and their relative errors, determined by the noise levels of ECE, are only 1%.

The X-mode reflectometry [17] signal at $\rho = 0.45$ increases after the TESPEL injection in all bandwidths (note that the fluctuation measurement by reflectometry is limited during the TESPEL ablation). The low frequency components (< 10kHz) grow abruptly. This abrupt response may be similar to that of the heat flux. On the other hand, the high frequency components (> 10kHz) grow slowly during 4-5ms from the TESPEL ablation and saturate. This temporal behavior is quite different from ones of the ∇T_e and the heat flux. To understand the correlations between the turbulence and the dynamics of heat transport, further information is required.

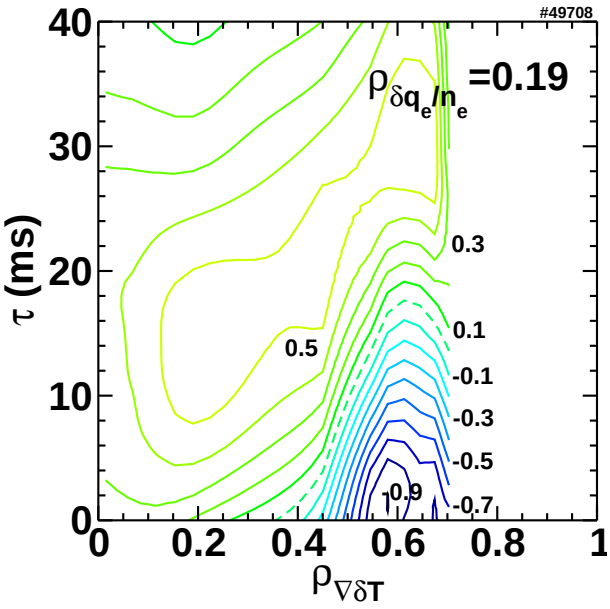

FIG. 2: Cross-correlation function between heat flux and temperature gradient. Contour maps of the cross-correlation function between $\delta q_e/n_e$ at $\rho = 0.19$ and the 21 $\nabla\delta T_e$ channels are shown in T_e rise case.

To obtain new physical insight into the non-local mechanism, the spatiotemporal correlation is derived. The cross-correlation functions between δq_e at $\rho = 0.19$ and the 21 $\nabla\delta T_e$ channels are calculated to demonstrate the existence of the long distance correlation in the non-local transport. The cross-correlation is defined as,

$$C_{f,g}(\rho_{\rm ref},\rho,\tau) = \langle f(\rho_{\rm ref},t)g(\rho,t+\tau)\rangle / \sqrt{\langle f^2(\rho_{\rm ref},t)\rangle\langle g^2(\rho,t)\rangle}, \quad (2)$$

where $f = \delta q_e/n_e(\rho,t)$, $g = \nabla\delta T_e(\rho,t)$, $\rho_{\rm ref} = 0.19$ and $\langle\rangle$ means temporal average, defined as $\langle h(t)\rangle = (T)^{-1}\int_0^T h(t)dt$. Figure 2 indicates that core ($\rho = 0.19$) heat flux is strongly coupled with the edge ($\rho = 0.58$) temperature gradient for a short time lag, and therefore, the existence of a long distance/non-local correlation between heat flux and temperature gradient is clarified. Moreover, the core to edge coupling shows a negative correlation (~ -1), i.e. a decrease in the flux with an increase in the gradient ($-\partial(q_e/n_e)/\partial\nabla T_e < 0$), which is often observed in transition phases [18]. The strong negative non-local correlation is reduced with an increase in the time lag. The correlation time, which is defined as peak width of time lag at half height, is 8 ms and is much longer than micro- and meso-scale times of $a/c_s \sim 1\mu s$ and $\sqrt{(a/\rho_i)(a/c_s)} \sim 30\mu s$.

4. Turbulent structures with a long radial correlation length

It is difficult to detect a certain type of fluctuation (e.g. zonal flows) by simply using the density fluctuation diagnostics due to the low level of density fluctuation components. Recent progress in the fluctuation diagnostics (e.g. HIBP) has clarified a nonlinear coupling of drift wave turbulence and structures. For example, the turbulent density fluctuations are modulated by the zonal flows through a parametric modulational instability [8]. Thus, density fluctuations have some information about structures, which can modulate them, in their envelope. In order to reveal

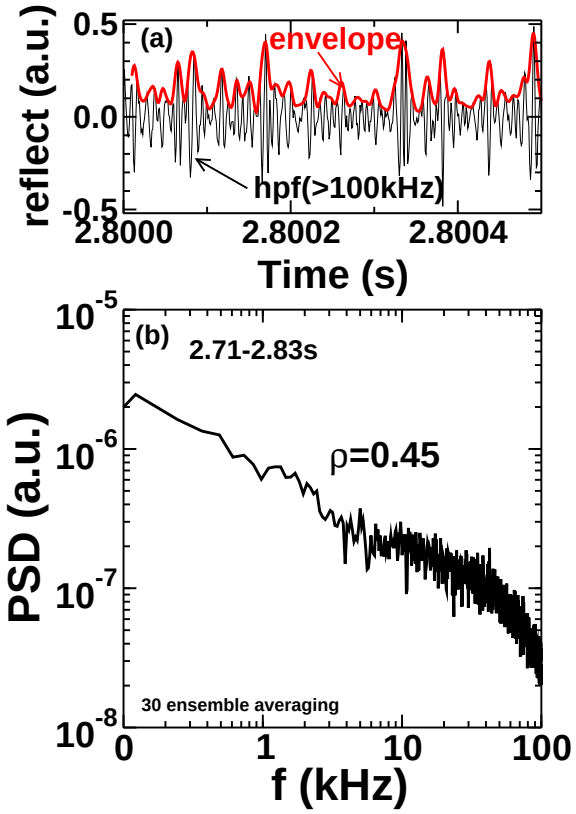

FIG. 3: (a) Time evolution of the high-pass filtered reflectometry signal (> 100kHz) at $\rho = 0.45$ and (b) Power spectrum densities of envelope at $\rho = 0.45$.

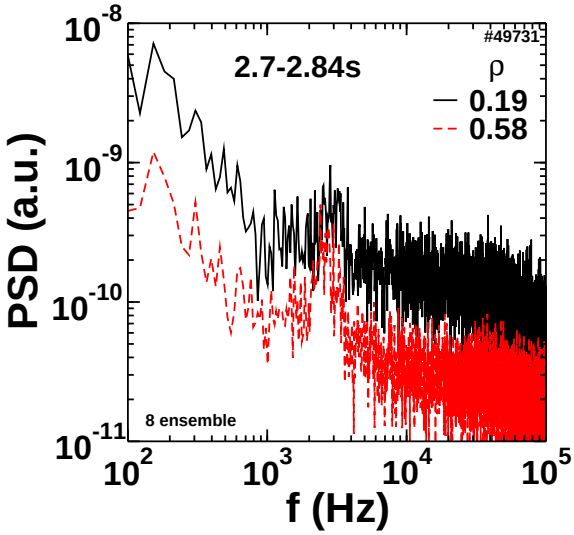

FIG. 4: Power spectral densities of the ECE signal at two different radii ($\rho = 0.19$ and $\rho = 0.58$).

the existence of such a modulator, the envelope of higher frequency components in the reflectometry signal, which is considered to be an index of the microscopic turbulence, is extracted by using Hilbert transform. Figure 3 shows a typical signal envelope and the power spectrum densities of the envelope at $\rho = 0.45$. The reflectometry signal data from the stationary state before the TESPEL injection are used for ensemble averaging to reduce the statistical error. As shown in Fig. 3(a), the envelope is modulated. The power spectrum density of the envelope at $\rho = 0.45$ indicates the existence of an amplitude modulator in the low frequency band (< 5kHz).

The low frequency components are also found in the ECE signals. A small peak at 1-5kHz and the broad-band components similar to the spectrum of the envelope of reflectometry signal are shown in Fig. 4. Here, only 8 ensembles are averaged due to a change in the baseline of ECE signals. Here we focus to a peak component. Figure 5 shows the cross-correlation functions of the low frequency component of ECE signals between two different radii, i.e. $f = \delta T_e(\rho, t)$, $g = \delta T_e(\rho, t)$ and $\rho_{ref} = 0.19$ in Eq. 2 (the reference point is $\rho = 0.19$ and therefore Fig. 5(a) means the auto-correlation function). The band-pass filter (1-5kHz) is applied to the ECE signals to extract the peak components only. The low frequency component of the core ($\rho = 0.19$) ECE signal correlates in the wide radial region of $\rho \leq 0.6$. Hence, this low frequency components may have a long distance correlation. The correlation length of this mode is similar to that observed in the flux-gradient correlation diagram shown in Fig. 2. The amplitude modulator observed in the density fluctuation may be thought to be identical with the low frequency components observed in the ECE signals because of the similarity of the

spectrum.

The modulator in the core region, thus, may have a radial correlation length, which is much longer than that of the meso-scale structures (e.g. 3 cm for zonal flows). Figure 6 shows the normalized amplitude structure of this mode. The normalized amplitude is large in the region of ρ = 0.3 – 0.5. In the employed magnetic configuration, there are low order rational surfaces (n/m = 1/2, 2/3, here n/m is toroidal/poloidal mode number) at ρ = 0.31 and 0.52 in the vacuum condition. A finite counter beam driven current (40-50 kA in this discharge) will shift the location of the rational surfaces outwardly. And a n/m = 1/2 mode with frequency of 2kHz is identified with the magnetic measurement system in this discharge. Thus the mode observed in ECE signals may be excited at the n/m = 1/2 rational surface. The n/m = 1/2 interchange mode has been observed by the ECE [19]. However, the mode amplitude is much smaller than reported one in this experimental condition and the mode structure is broader than a calculated ideal interchange mode structure. Further fact that the phase delay indicates a outward propagation from core ρ = 0.19 to edge ρ = 0.58. Fluctuation of the long wavelength mode excited from background micro fluctuation [20] is a possible candidate. Fluctuations with long radial correlation length can cause edge-core coupling of heat transport. Further study is required to identify the observed mode. Analysis of the broad-band components in the low frequency band (< 1kHz) and identification of non-linear coupling between turbulent modes by using of bi-spectral analysis will be also the object of future work.

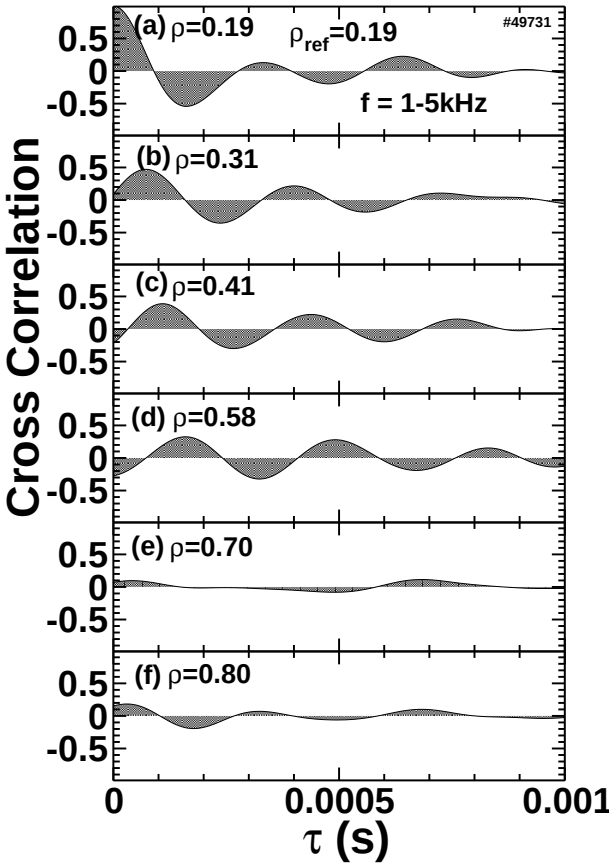

FIG. 5: Cross-correlation functions of the low frequency component (1-5 kHz) of ECE signals between six different radii. The δT_e at ρ = 0.19 is used as a reference. Note the band-pass filter (1-5 kHz) is applied to the ECE signal.

5. Summary

In summary, we investigated the radial correlation scale of heat transport and micro- to meso- or macro-scale coupling of ECE and turbulent density fluctuations in LHD plasmas, where the non-local transport phenomena are observed. The experimental results show the following non-local electron heat transport features. (i) The radial correlation scale of heat transport is obtained by using the cross-correlation function between perturbations of heat flux and temperature gradient at different radii. (ii) An observed strong correlation between the core heat flux and the edge temperature gradient in the non-local T_e rise indicates a radial correlation scale of heat transport is much longer than the micro-turbulence correlation length. (iii) the envelope of the density

turbulence indicates the existence of an amplitude modulator of the density turbulence with low frequency (< 5kHz). (iv) the ECE fluctuation with low frequency (1 – 5kHz) shows the long (order of the minor radius) distance radial correlation.

The low frequency turbulence modulator may have meso- or macro- structure. Interaction of turbulence and transport over long distances is one of the candidate to explain the non-local transport mechanisms. Excitation mechanisms of the long correlated turbulence structures and couplings between the transport and the turbulence modulator will be clarified in future work.

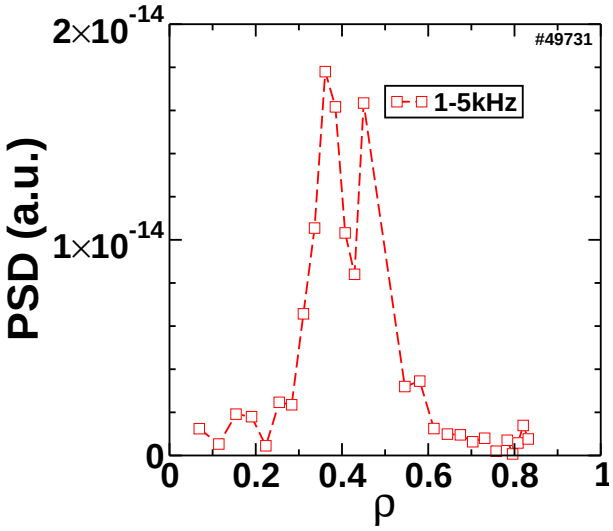

FIG. 6: Radial profile of the low frequency component (1-5 kHz) of ECE signals. There are low order rational surfaces at ρ = 0.31 *and 0.52 in the vacuum condition.*

Acknowledgments

We thank Professor O. Motojima for his continuous encouragement and Professor P. H. Diamond for useful discussion. We are grateful to the technical group for their excellent support. This work is partly supported by a grant-in-aid for Specially-Promoted research (16002005), by the Grant-in-Aid for Scientific Research (C) and by the collaboration programs of NIFS (NIFS07KOAP017).

References

[1] B. P. van Milligen *et al* , Nucl. Fusion **42** (2002) 787

[2] V. V. Parail *et al* , Nucl. Fusion **37** (1997) 481

[3] U. Stroth *et al* , Plasma Phys. Control. Fusion **38** (1996) 1087

[4] G. R. McKee *et al* , Nucl. Fusion **41** (2001) 1235

[5] R. V. Budny *et al* , Phys. Plasmas **7** (2000) 5038

[6] M. N. Rosenbluth and F. L. Hinton, Phys. Rev. Lett. **80** (1998) 724

[7] Z. Lin *et al* , Science **281** (1998) 1835

[8] P. H. Diamond *et al* , Plasma Phys. Control. Fusion **47** (2005) R35

[9] M. Yagi *et al* , Plasma Fusion Res. **2** (2007) 0251

[10] S. Inagaki *et al* , Plasma Phys. Control. Fusion **48** (2006) A251

[11] N. Tamura *et al* , Nucl. Fusion **47** (2007) 449

[12] S. Sudo *et al* , Plasma Phys. Control. Fusion **44** (2002) 129

[13] K. W. Gentle *et al* , Phys. Rev. Lett. **74** (1995) 3620

[14] P. Mantica *et al* , Phys. Rev. Lett. **82** (1999) 5048

[15] K. Tanaka *et al* , Nucl. Fusion **46** (2006) 110

[16] K. Kawahata *et al* , Rev. Sci. Instrum. **74** (2003) 1449

[17] T. Tokuzawa *et al* , Proc. 31st EPS Conf. on Plasma Physics **1** (2004) P–5.114

[18] K. Ida *et al* , Phys. Rev. Lett. **96** (2006) 125006

[19] A. Isayama *et al* , Plasma Phys. Control. Fusion **48** (2006) L45

[20] S.-I. Itoh and K. Itoh, Plasma Phys. Control. Fusion **43** (2001) 1055